

Polymer Chemistry

Accepted Manuscript



This is an *Accepted Manuscript*, which has been through the Royal Society of Chemistry peer review process and has been accepted for publication.

Accepted Manuscripts are published online shortly after acceptance, before technical editing, formatting and proof reading. Using this free service, authors can make their results available to the community, in citable form, before we publish the edited article. We will replace this *Accepted Manuscript* with the edited and formatted *Advance Article* as soon as it is available.

You can find more information about *Accepted Manuscripts* in the [Information for Authors](#).

Please note that technical editing may introduce minor changes to the text and/or graphics, which may alter content. The journal's standard [Terms & Conditions](#) and the [Ethical guidelines](#) still apply. In no event shall the Royal Society of Chemistry be held responsible for any errors or omissions in this *Accepted Manuscript* or any consequences arising from the use of any information it contains.

Cite this: DOI: 10.1039/c0xx00000x

www.rsc.org/xxxxxx

ARTICLE TYPE

CO₂-driven vesicles to micelle regulation of amphiphilic copolymer: random versus block strategy

Hanbin Liu,^{ac} Zanru Guo,^{ac} Shuai He,^{ac} Hongyao Yin,^{ac} Chenhong Fei^{ac} and Yujun Feng^{*ab}

Received (in XXX, XXX) Xth XXXXXXXXX 20XX, Accepted Xth XXXXXXXXX 20XX

DOI: 10.1039/b000000x

Precise morphologic controlling over self-assemblies is attractive due to their promising applications, especially in biotherapy. Block copolymer is the common choice for the morphologic control, since the geometry of self-assemblies can be easily predicted by the hydrophilic volume fraction. However, random copolymers are rarely taken into consideration. Here, starting from the same hydrophilic segment poly(ethylene oxide) (PEO), and using CO₂-responsive 2-(diethylamino) ethyl methacrylate (DEAEMA) and hydrophobic styrene (St), we designed and synthesized a random and an entire block copolymer with similar polymerization degree but different monomer sequence: PEO₄₅-*b*-(DEAEMA₉₀-*r*-St₆₆) (**P_r**) and PEO₄₅-*b*-DEAEMA₉₃-*b*-St₆₆ (**P_b**). In aqueous solution, the two polymers both aggregate into vesicles. Upon the CO₂-stimulus, however, the vesicle of random copolymer **P_r** transforms into spherical micelle, while that of triblock copolymer **P_b** shows an expansion instead of morphologic transition. The restricted hydration in random structure of **P_r** accounts for such a morphologic transition, and the random strategy in polymer design might be useful in the self-assembly regulation.

Introduction

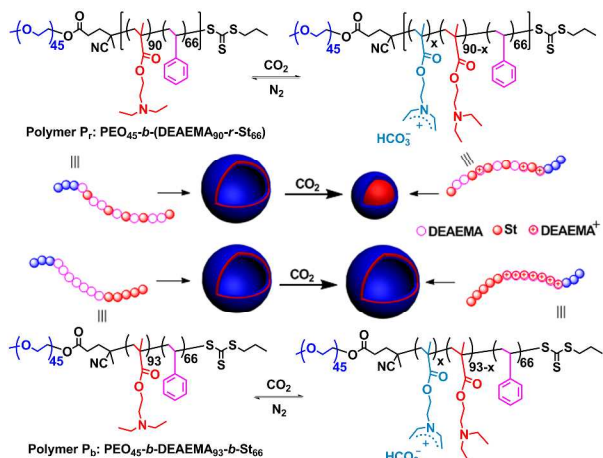
Polymer vesicles are nanoscale sacs enclosed with a polymeric membrane,¹ which are more robust and much easier to be decorated with reactive groups compared with lipid-based vesicles.² Thus the stimuli-responsive polymeric vesicles have attracted much attention with endless potential applications, ranging from drug delivery to enzymatic nano-reactors.²⁻⁴ Upon a specific stimulus, the transformation from vesicle to individual chains has been extensively reported.^{3,5-11} However, precise morphologic controlling over vesicle to other geometries, such as spherical micelles, cylinders, or worm-like micelles, remains a subject of intense research interest.^{12,13} The morphologic regulation can be used to mimic and investigate some organismal behaviours, such as the volume tuning, unfolding, and endocytosis of organelles, which would help us understand biological autonomous motions in nature.¹⁴ Moreover, the morphologic transition has been proposed to be useful in controlled release and sensing applications.³

Nevertheless, the triggers reported to date for vesicular regulation have been restricted to temperature,^{5,12,15} pH,^{13,16,17} light,^{18,19} and selective recognition.²⁰ Compared with these traditional stimuli, CO₂ as a novel trigger is easily-removing and free of contamination since the produced bicarbonate salt is unstable, thus endowing the “smart” system with a better reversibility.²¹⁻²⁵ Furthermore, CO₂ is an endogenous metabolite (the dissolved CO₂ in plasma is normally about 1.2 mM²⁶) with non-toxic nature, as well as good biocompatibility and membrane permeability,²¹⁻²⁵ processing great potential application in biotherapy.^{14,27,28} Very recently, CO₂ has been used to regulate

the polymer-based aggregate morphology as well. Both Yuan and Zhao group^{27,29,30} developed vesicles which undergo an interesting “CO₂-breathing” behaviour. Subsequently, Zhao and co-workers²⁸ reported a shape transformation upon CO₂-stimulus from microscopic tubules to submicroscopic vesicles and then nano-micelles. Noteworthy, these CO₂-driven morphologic manipulations are realized based on block copolymers. But it is well known that the synthetic processes for block structure are always tedious and time-consuming, involving multistep copolymerization and post-polymerization treatment. Random copolymers, on the other hand, can be achieved from diverse components in a single polymerization step.³¹⁻³³ Furthermore, the random strategy might result in a special morphology,^{34,35} taking the rare bowl-shape aggregates as an example, which is fabricated with a random copolymer of poly(styrene-*co*-methacrylic acid) by Eisenberg and his coworkers.³⁶ Therefore, it is interesting to investigate whether the CO₂-driven vesicle to spherical micelle regulation can be realized with a random strategy. Besides, to the best of our knowledge, no report so far deals with the direct vesicle to spherical micelle manipulation upon the stimulus of CO₂.

Here in this work, resorting to the ester condensation of chain transfer agent (CTA) with carboxylic acid (-COOH) and PEO with one end hydroxyl (-OH), we firstly synthesized a macromolecular chain transfer agent *macro*-PEO₄₅; then using CO₂-responsive monomer 2-(diethylamino) ethyl methacrylate (DEAEMA) and hydrophobic monomer styrene (St), we designed and synthesized a copolymer PEO₄₅-*b*-(DEAEMA₉₀-*r*-St₆₆) (**P_r**) with a random strategy and a triblock copolymer PEO₄₅-*b*-DEAEMA₉₃-*b*-St₆₆ (**P_b**) as a contrast with comparable

polymerization degree of DEAEEMA and St. The same water soluble block PEO₄₅ makes a promise for them to aggregate into vesicle in aqueous solution, since the DEAEEMA is also hydrophobic as St before CO₂-stimulus. After the treatment of CO₂, a different morphologic change has been demonstrated (Scheme 1), which is caused by their distinct molecular structure and the resulting different protonation of tertiary amine groups.



Scheme 1 CO₂-responsive copolymers with random structure (top, P_r) or entire triblock structure (bottom, P_b), and schematic illustration of the different protonation as well as morphologic change upon the CO₂ stimulus (middle).

Experimental

Materials

The monomer 2-(diethylamino) ethyl methacrylate (DEAEEMA, Aldrich, 99%) is passed through an activated basic alumina column, while styrene (St, Sigma-Aldrich, ≥99%) is distilled under reduced pressure to remove the inhibitors. *N*-(3-dimethylaminopropyl)-*N'*-ethylcarbodiimide hydrochloride crystalline (EDAC), 4-(dimethylamino) pyridine (DMAP, ≥99%), 4,4'-Azobis(4-cyanovaleric acid) (ACVA, ≥98.0%), and poly(ethylene glycol) methyl ether (mPEG-2000, or PEO, M_n ~2,000, flakes), were purchased from Sigma-Aldrich and used as received. The organic solvents with A.R. grade were obtained from Guanghua Sci-Tech Co., Ltd. (Guangdong, China) without further treatment unless otherwise specified. The deionized water (conductivity, κ=7.9 μS·cm⁻¹) used in the dialysis process was treated by the ultrapure water purification system (CDUPT-III type, Chengdu Ultrapure Technology Co., Ltd., China). The CTA, 4-cyano-4-thiothiopropylsulfanylpentanoic acid (CTPPA), for RAFT polymerization, was synthesized according to the previously reported procedures.^{37,38}

Characterization

¹H NMR spectra were recorded at 25 °C on a Bruker AV300 NMR spectrometer at 300 MHz. The chemical shifts (δ) are reported in parts per million (ppm) with reference to the internal standard protons of tetramethylsilane (TMS). The molecular weight and the molecular weight distribution of the polymers were determined by a gel permeation chromatography (GPC) system equipped with a Waters 515 pump and a 2410 detector. THF was used as the eluent at a flow rate of 1.0 mL·min⁻¹ at 40

°C. Monodisperse polystyrene was used as the standard to generate the calibration curve. The transmittance of the aggregate solution was recorded on a UV-4802 double beam spectrophotometer (Unico Instrument Co., China) at room temperature at the wavelength of 550 nm. Dynamic light scattering (DLS) measurements were performed on a Malvern Zetasizer Nano-ZS90 apparatus equipped with a He-Ne laser operated at 633 nm. All samples were measured at a scattering angle of 90° with polymer concentration of 1.0 g·L⁻¹ at 25 °C. Transmission electron microscopy (TEM) observation was conducted on a Hitachi H600 electron microscope instrument operated at an acceleration voltage of 75 kV. The specimens were prepared by placing one drop of sample on copper grids coated with polyvinyl formal film and then stained by 0.2 wt% phosphotungstic acid aqueous solution. Cryo-TEM observations were performed on a FEI Titan Krios cryo-microscope (FEI, U.S.A) at an acceleration voltage of 300 kV. A drop of the micelle solution was deposited on a carbon-coated copper grid. The excess solution was absorbed with filter paper, and the specimen was rapidly plunged into liquid ethane and transferred to liquid nitrogen where it was kept until use. The images were recorded digitally with a 2K×2K Gatan Ultrascan 894 CCD camera. The conductivity of aggregate solution was determined by an FE30 conductometer (Mettler Toledo, USA) at room temperature. The pH variation was monitored by a Sartorius basic pH meter PB-10 (±0.01) calibrated with standard buffer solutions. To measure the pK_a of the copolymers in aqueous solution, 5 mL polymer solution was titrated with 0.002 mol·L⁻¹ hydrochloric acid calibrated by NaOH, while the pH was continuously monitored with the pH meter. The pH corresponding to the half of the equivalence was taken as the pK_a value.³⁰

Synthesis of the macromolecular chain transfer agent *macro*-PEO₄₅

Dichloromethane (DCM) was dried with CaH₂ and then refluxed to be used as the solvent for the reaction. The chain transfer agent CTPPA (0.554 g, 2.0 mmol), mPEG-2000 (2.0 g, 1.0 mmol), EDAC (0.767 g, 4.0 mmol) and DMAP (0.244 g, 2.0 mmol) dissolved in 50 mL dried DCM were added into a 100-mL round bottom flask equipped with a magnetic bar stirring for 48 h at room temperature after deoxygenating by bubbling Ar gas for 15 min. The reaction mixture was concentrated and precipitated in -72 °C *n*-hexane (in the bath of acetone and dry ice mixture) for three times, and then washed with diethyl ether for three times. Finally, a yellow powder was obtained after lyophilisation (1.8 g, yield: 90%). ¹H NMR (δ, ppm, CDCl₃; Fig. S1): 3.62 (-CH₂CH₂O-), 3.35 (-OCH₃, -SCH₂-), 2.38–2.72 (-OOCCH₂CH₂-), 1.85 (-C(CH₃)(CN)-), 1.67–1.83 (-SCH₂CH₂CH₃), 0.97–1.02 (-SCH₂CH₂CH₃).

Preparation of random copolymer P_r, PEO₄₅-b-(DEAEEMA_{90-r}-St₆₆)

Using the above synthesized macromolecular RAFT agent, the random copolymer P_r, PEO₄₅-b-(DEAEEMA_{90-r}-St₆₆), was synthesized as follows: the *macro*-PEO₄₅ (0.3 g, 0.132 mmol), ACVA (7 mg, 0.026 mmol), DEAEEMA (3.2 g, 17.2 mmol), St (0.48 g, 4.62 mmol) and 2 mL of dried THF were added into a reaction tube equipped with a magnetic bar. After deoxygenizing by three freeze-pump-thaw cycles, the reaction mixture was

stored at 70 °C for 10 h with magnetic stirring.

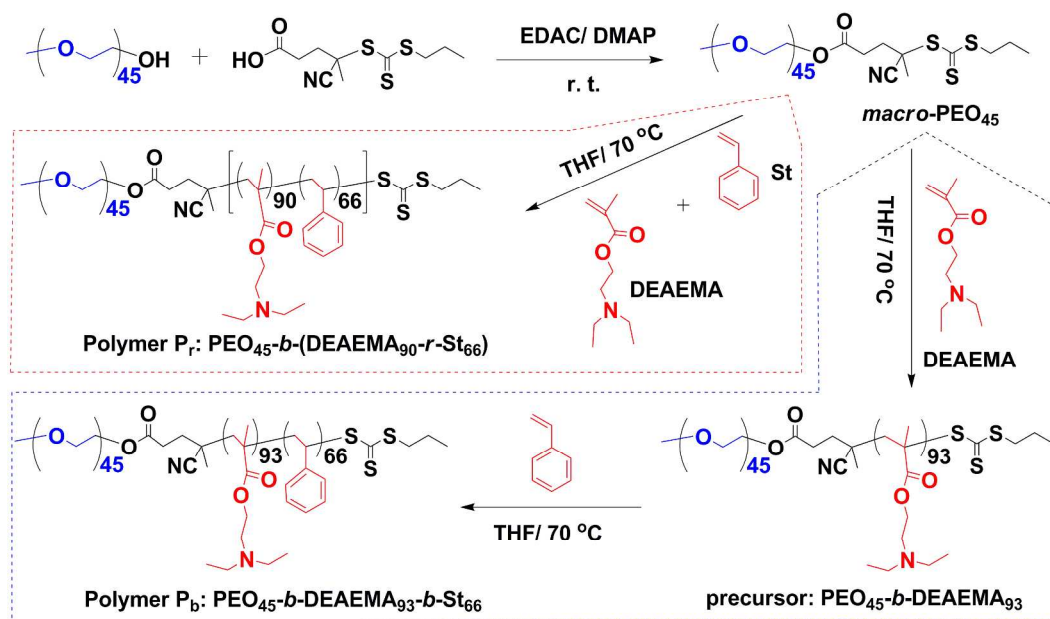


Fig. 1 Synthesis route of the copolymer P_r and P_b .

5 The polymerization was terminated by freezing in liquid nitrogen. Finally, the product was obtained after precipitation in *n*-hexane and lyophilization (yield: 3.2 g). 1H NMR (δ , ppm, CD_2Cl_2 ; Fig. S2): 6.79–7.31 ($-C_6H_5$), 3.75–4.19 ($-COOCH_2CH_2N(CH_2CH_3)_2$), 3.60 ($-CH_2CH_2O-$), 3.37 ($-OCH_3$), 3.27 ($-SCH_2-$), 2.21–2.72 ($-OOCCH_2CH_2-$, $-COOCH_2CH_2N(CH_2CH_3)_2$), 1.32–1.81 ($-CH_2CH_3CH_2-$, $CNCH_3CH_2-$, $-SCH_2CH_2CH_3$), 0.74–1.20 ($-N(CH_2CH_3)_2$, $-CH_2CH_3CH_2-$, $-SCH_2CH_2CH_3$). From the peak area ratio of PEO_{45} (peak *b*, Fig. S2) and the DEAEEMA moieties (peak *h*, Fig. S2) and St moieties (peak *l*, Fig. S2), it is easy to calculate the polymerization degree according to equations (1) and (2) shown in electronic supporting information (ESI), from which we obtained $DP_{DEAEEMA,NMR}=90$ and $DP_{St,NMR}=66$, respectively; And the molecular weight is $M_{n,NMR}=2.6 \times 10^4$ g·mol $^{-1}$, $M_{n,GPC}=2.8 \times 10^4$ g·mol $^{-1}$, $M_w/M_n=1.29$.

20 Preparation of diblock precursor $PEO_{45}-b-DEAEEMA_{93}$

Using the macromolecular RAFT agent, the diblock precursor $PEO_{45}-b-DEAEEMA_{93}$ was synthesized as follows: the $macro-PEO_{45}$ (0.3 g, 0.132 mmol), ACVA (7 mg, 0.026 mmol), DEAEEMA (3.2 g, 17.2 mmol), 4 mL of dried THF were added into a reaction tube equipped with a magnetic bar. After deoxygenizing by three freeze-pump-thaw cycles, the reaction mixture was stored at 70 °C for 18 h with magnetic stirring. The polymerization was terminated by freezing the mixture in liquid nitrogen. Finally, the product was obtained after precipitation in *n*-hexane and lyophilization (yield: 2.5 g; conversion: 70%). 1H NMR (δ , ppm, CD_2Cl_2 ; Fig. S3): 3.75–4.19 ($-COOCH_2CH_2N(CH_2CH_3)_2$), 3.60 ($-CH_2CH_2O-$), 3.37 ($-OCH_3$), 3.27 ($-SCH_2-$), 2.21–2.72 ($-OOCCH_2CH_2-$, $-COOCH_2CH_2N(CH_2CH_3)_2$), 1.32–1.81 ($-CH_2CH_3CH_2-$, $CNCH_3CH_2-$, $-SCH_2CH_2CH_3$), 0.74–1.20 ($-N(CH_2CH_3)_2$, $-CH_2CH_3CH_2-$, $-SCH_2CH_2CH_3$). From the peak area ratio of PEO_{45} (peak *b*, Fig. S3) and the DEAEEMA moieties (peak *h*, Fig. S3), the calculated polymerization degree is $DP_{DEAEEMA,NMR}=93$,

and the corresponding molecular weight is $M_{n,NMR}=1.95 \times 10^4$ g·mol $^{-1}$.

Preparation of triblock copolymer P_b , $PEO_{45}-b-DEAEEMA_{93}-b-St_{66}$

Using the above diblock precursor $PEO_{45}-b-DEAEEMA_{93}$ as a new macromolecular RAFT agent, the triblock copolymer P_b , $PEO_{45}-b-DEAEEMA_{93}-b-St_{66}$ was synthesized as follows: the $PEO_{45}-b-DEAEEMA_{93}$ (0.3 g, 0.015 mmol), ACVA (1 mg, 0.003 mmol), St (0.26 g, 2.38 mmol), 2 mL of dried THF were added into a reaction tube equipped with a magnetic bar. After deoxygenizing by three freeze-pump-thaw cycles, the reaction mixture was stored at 70 °C for 36 h with magnetic stirring. The polymerization was terminated by freezing the mixture into liquid nitrogen. Finally, the product was obtained after precipitation in *n*-hexane and lyophilization (yield: 0.4 g; conversion: 40%). 1H NMR (δ , ppm, CD_2Cl_2 ; Fig. S4): 6.79–7.31 ($-C_6H_5$), 3.75–4.19 ($-COOCH_2CH_2N(CH_2CH_3)_2$), 3.60 ($-CH_2CH_2O-$), 3.37 ($-OCH_3$), 3.27 ($-SCH_2-$), 2.21–2.72 ($-OOCCH_2CH_2-$, $-COOCH_2CH_2N(CH_2CH_3)_2$), 1.32–1.81 ($-CH_2CH_3CH_2-$, $CNCH_3CH_2-$, $-SCH_2CH_2CH_3$), 0.74–1.20 ($-N(CH_2CH_3)_2$, $-CH_2CH_3CH_2-$, $-SCH_2CH_2CH_3$). From the peak area ratio of PEO_{45} (peak *b*, Fig. S4) and the DEAEEMA moieties (peak *h*, Fig. S4) and St moieties (peak *l*, Fig. S4), the polymerization degree can be calculated and is $DP_{St,NMR}=66$, and thus the corresponding molecular weight is $M_{n,NMR}=2.6 \times 10^4$ g·mol $^{-1}$, $M_{n,GPC}=2.9 \times 10^4$ g·mol $^{-1}$, $M_w/M_n=1.30$.

65 Preparation of assemblies

The assemblies were prepared with the typical procedure as follows: 20 mg polymer was dissolved into 10 mL tetrahydrofuran (THF) and stirred for several hours, then dialyzed against deionised water for 3 days to exclude the organic solvent. The solution was diluted to 20 mL, yielding the aqueous solution of aggregates with a concentration of 1.0 g·L $^{-1}$. Further

experiments involving conductivity, pH, responsiveness to CO₂ and TEM observation are all performed upon these aggregate solutions.

Results and discussion

After synthesis the macromolecular chain transfer agent *macro*-PEO₄₅ with an ester condensation reaction, the copolymer **P_r** and **P_b** were both polymerized via RAFT polymerization. The detailed synthesis route is depicted in Fig. 1. To synthesize the random copolymer **P_r**, we added the DEAEEMA and St at the same feeding, obtaining product in one pot for about 10 h reaction. However, whether the product appears as random structure is still puzzling. There is no reported value of reactivity ratio for St/DEAEEMA copolymerization. But the reactivity ratio of St/DMAEMA is obtained from the literature,³⁹ showing as $r_1 = 0.22$ and $r_2 = 0.42$, where the subscript 1 refers to styrene. The DMAEMA refers to 2-(dimethylamino)ethyl methacrylate, which has similar structure with DEAEEMA used in the present work, so these parameters can be used as a replacement. Given the $r_2 < 1$ and $r_2 < 1$, it is reasonable to conclude that the product is a random structure. Furthermore, armed with $r_{St} = 0.22$ and $r_{DEAEEMA} = 0.42$, the average sequence length of St and DEAEEMA can be calculated as 1.06 and 2.56, respectively (detail calculation is depicted in Electronic Supporting Information, ESI). It means every one St unit locates in 3 DEAEEMA units in general, implying only the DEAEEMA unit where the sequence length is over 3 can react with CO₂. On the other hand, to prepare the triblock counterpart **P_b**, we have to synthesize a diblock precursor PEO₄₅-*b*-DEAEEMA₉₃ with additional post-polymerization treatments, which is really more complicated than the preparation of random copolymer **P_r**.

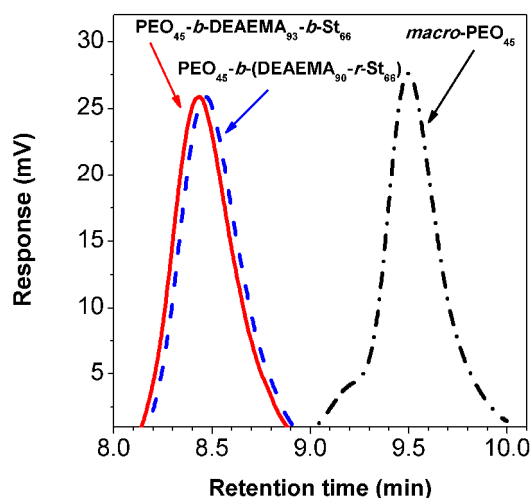


Fig. 2 GPC chromatogram for the copolymers, **P_r** [PEO₄₅-*b*-(DEAEEMA₉₀-*r*-St₆₆)], **P_b** (PEO₄₅-*b*-DEAEEMA₉₃-*b*-St₆₆), and RAFT agent *macro*-PEO₄₅.

The ¹H NMR characterizations of the above-mentioned polymers are shown in Figs. S1–S4 of ESI. From the ¹H NMR spectra, we can estimate the M_n of **P_r** and **P_b**, both of which have the same molecular weight as 2.6×10^4 g·mol⁻¹. The M_n of **P_r** and **P_b** from GPC measurement is also comparable, and both of their molecular weight distribution M_w/M_n is around 1.30, which is less than 1.40 and can be accepted for a controlled radical

polymerization.^{40,41} Compared with the GPC curve of *macro*-PEO₄₅, the curves of **P_r** and **P_b** display a large shift without shoulder peak, indicating the complete initiation of *macro*-PEO₄₅ as a chain transfer agent (Fig. 2).

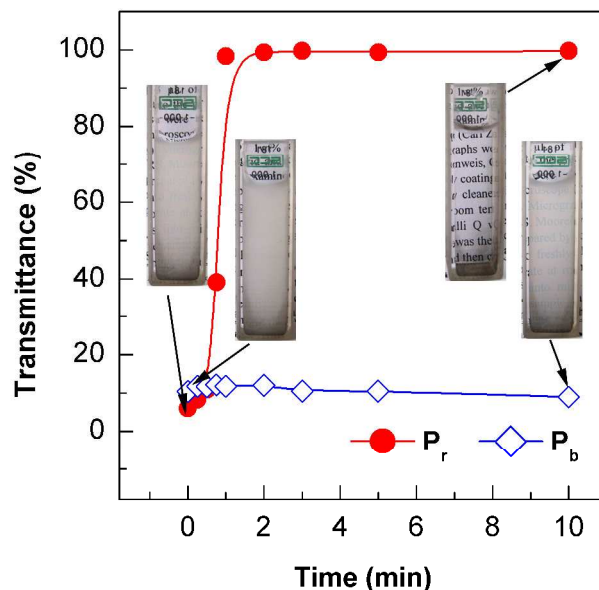


Fig. 3 Transmittance change of **P_r** and **P_b** self-assembly solution as a function of time when CO₂ is bubbled with a fixed flow rate of approximately 15 mL·min⁻¹. The transmittance was detected at the 50 wavelength of 550 nm, where the polymer concentration is 1.0 g·L⁻¹.

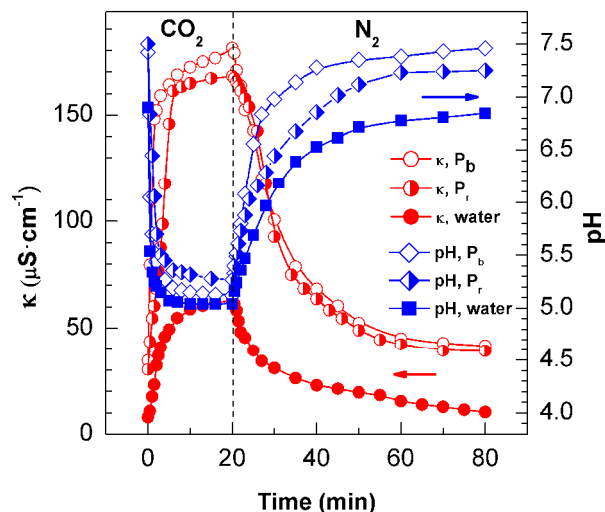


Fig. 4 Conductivity (κ) and pH variation of aggregate solution of polymer **P_r**, **P_b** and pure water as a function of time under alternative stimuli of CO₂ and N₂. The measurements were conducted at room temperature with a fixed gas flow rate at approximately 15 mL·min⁻¹. The polymer concentration of **P_r** and **P_b** is 1.0 g·L⁻¹.

After obtaining the copolymer **P_r** and **P_b** with different hydrophobic structures, we prepared the self-assembly solution with assistance of organic solvent THF, and quickly discovered their different turbidity changes upon the stimulus of CO₂. As showing in Fig. 3, the original solution of random copolymer **P_r** is absolutely opaque before CO₂ aeration, but becomes transparent only after 2 min of CO₂ treatment. The corresponding transmittance increases from 6% to 99% during this period and then maintains at this value. But for the triblock copolymer **P_b**, its

aqueous solution is always opaque before and after CO₂ treatment (Fig. 3) and the transmittance stays nearly unchanged at about 10%. It is well known that the colloidal solution turbidity has a positive correlation with the colloidal size,²⁸ so large aggregates are expected for the opaque solution, while the transparent solution implies self-assemblies with small size (this point will be discussed further in the following).

To further confirm the CO₂-responsiveness of the copolymers **P_r** and **P_b**, the variation of conductivity and pH of polymer solutions was monitored during alternately bubbling CO₂ and N₂. As shown in Fig. 4, the conductivity (κ) of **P_r** aqueous solution increases perpendicularly from 30.3 to 161.2 $\mu\text{S}\cdot\text{cm}^{-1}$ in 6 min, and finally ascends to the maximum of 168.1 $\mu\text{S}\cdot\text{cm}^{-1}$ during CO₂ bubbling, indicating the production of bicarbonate ions in solution.^{42,43} Correspondingly, the pH value drops from 7.50 to 5.27, suggesting the protonation of the tertiary amine groups of the DEAEMA unit in **P_r**. Similarly, the pH of its triblock counterpart **P_b** decreases from 7.42 to 5.12 and the conductivity increases from 34.6 to 181.1 $\mu\text{S}\cdot\text{cm}^{-1}$ (Fig. 4), both comparable with the above random copolymer. The pH and conductivity of pure water shows similar variation tendency. But the maximum conductivity can only reach 63.2 $\mu\text{S}\cdot\text{cm}^{-1}$, which is much less than that of **P_r** and **P_b** in solution, indicating over 65% of pH reduction is caused the CO₂ responsive polymers excluding the influence of water.

Given the previous literature has established a method to determine the precise value of protonated degree (δ) with $\text{p}K_{\text{a}}$ and pH,³⁰ here we also detected the $\text{p}K_{\text{a}}$ values of **P_r** and **P_b** by titration with 0.002 mol·L⁻¹ HCl solution, indicating 5.0 for the random polymer **P_r**, while 6.7 for the triblock counterpart **P_b** (Fig. S5). As shown in Fig. 5, the calculated δ of **P_r** is 0.3% before treatment of CO₂, and then gradually increases to 35% after aeration of CO₂ for 20 min. In sharp contrast, the δ of **P_b** increases from 16% to 97% in four minutes of CO₂-bubbling and then keeps at this value for 20 min, indicating the much higher and easier protonation of DEAEMA in block structure than that in random copolymer.

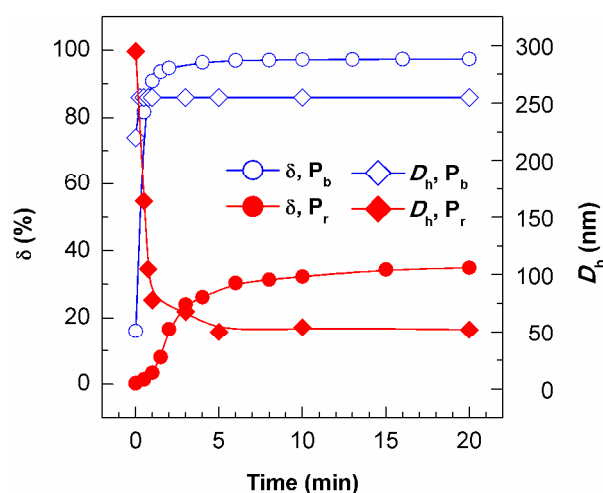


Fig. 5 The change of protonated degree (δ) and average hydrodynamic diameter (D_{h}) of the aggregates during CO₂ bubbling for the random copolymer **P_r**, and triblock counterpart **P_b**. The concentration of polymer is 1.0 g·L⁻¹, and the flow rate is kept at approximately 15 mL·min⁻¹.

To investigate whether the different protonation would lead to

distinct aggregate change, Dynamic light scattering (DLS) measurement is employed to determine the aggregate size when CO₂ is bubbled into the solution. For the random copolymer **P_r**, the average hydrodynamic diameter (D_{h}) is approximately 295 nm (Fig. 5) before aeration of CO₂, and rapidly drops to 78 nm after bubbling CO₂ for 1 min, then decreases to the minimum of 50 nm after the aeration of CO₂ for 5 min and remains stable up to 20 min, when the flow rate of CO₂ is kept at approximately 15 mL·min⁻¹. Besides, the polydispersity index (PDI) reduces from 0.52 to 0.23, indicating the size of the assemblies becomes more uniform. On the contrary, the D_{h} of the triblock copolymer **P_b** aggregates is approximately 190 nm before bubbling of CO₂, then increases to 255 nm in less than 1 min of CO₂ treatment and remains unchanged (Fig. 5) with a fixed PDI of around 0.16 in the following 20 min of CO₂ bubbling, demonstrating the aggregate size of **P_b** has an increase rather than a significant decrease as **P_r** in this period. This expansion might be caused by the kinetically trap of St portion in the vesicular formation of triblock copolymer **P_b** (Fig. S6). It may be also caused by the easier protonation of DEAEMA moieties than that of **P_r**. And the significant size decrease of **P_r** is in agreement with the appearance change from opaque to transparent (transmittance from 6% to 99%) of the **P_r** aqueous solution, implying a morphologic transformation. Noticeably, it is interesting to investigate the relationship of the δ and the D_{h} during CO₂ treatment. As shown in Fig. 5, for the random copolymer **P_r**, the δ increases from 0.3% to 35% and the D_{h} decreases from 295 to 50 nm in the first five minutes and then remains unchanged. These variations occur in the same pace, demonstrating that the parameters are all caused by the reaction of tertiary amine groups with CO₂, since the δ value is derived from pH, and the pH variation is a direct evidence of the protonation. While for its triblock counterpart **P_b**, the increase of δ and D_{h} finishes in the first two minutes, being indicative of the same pace as well. The difference lies in the higher δ and almost steady D_{h} value comparing with that of **P_r**, implying the invariance of aggregates morphology.

In order to verify the aggregate change predicted by transmittances and size measurements, transmission electron microscopy (TEM) was firstly used to visualize the aggregate morphologies. Stained with phosphotungstic acid, the aggregate of the random copolymer **P_r** appears as typical vesicle with clear contrast between the dark periphery and hollow center (Fig. 6a) in the absence of CO₂. Statistical calculation from the TEM image (Fig. 6a) gives the average diameter of approximately 244 nm. While after the treatment of CO₂, the aggregate appears as spherical micelle (Fig. 6b, the hydrophobic core cannot be stained by hydrophilic phosphotungstic acid so appears as white) with an average diameter of about 52 nm. This vesicle to spherical micelle morphologic transition is in accordance with the size decrease from 295 to 50 nm demonstrated with DLS measurement (Fig. 5). Cryogenic transmission electron microscopy (cryo-TEM) was further employed to study the morphology to avoid the artifacts linked to staining within the TEM sample preparation. The self-assembly of the copolymer **P_r** shows as vesicle with the average diameter of 253 nm (Fig. 6c and 6d, 6d is an enlarged view) before aeration of CO₂, and uniform spherical micelle (Fig. 6e, showing as black particle

since the cryo-TEM is not stained) with average diameter of 35 nm after reaction with CO₂, which is in good line with the TEM observation.

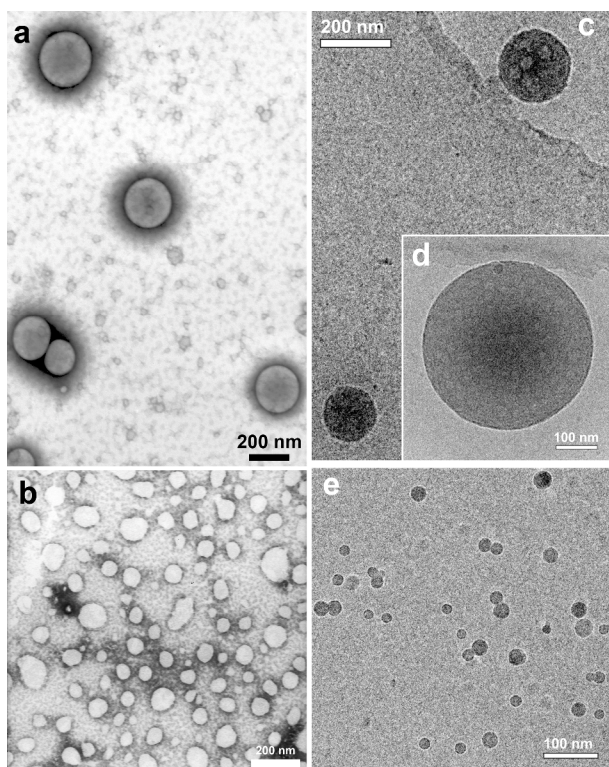


Fig. 6 TEM (a, b; stained with 0.2 wt% phosphotungstic acid) and cryo-TEM (c, d and e; free of staining) images of the assemblies for random copolymer **P_r**. (a), (c) and (d), before CO₂ bubbling; (b) and (e), after CO₂ bubbling. Bars: (a), (b) and (c), 200 nm; (d) and (e), 100 nm.

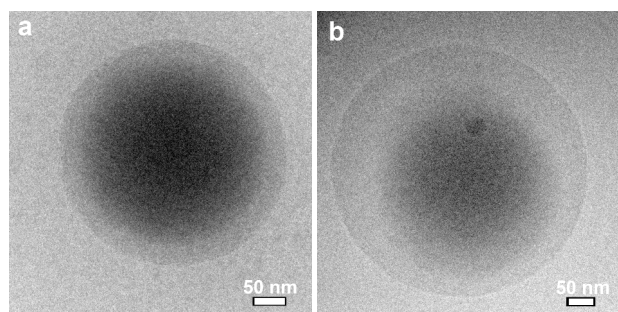
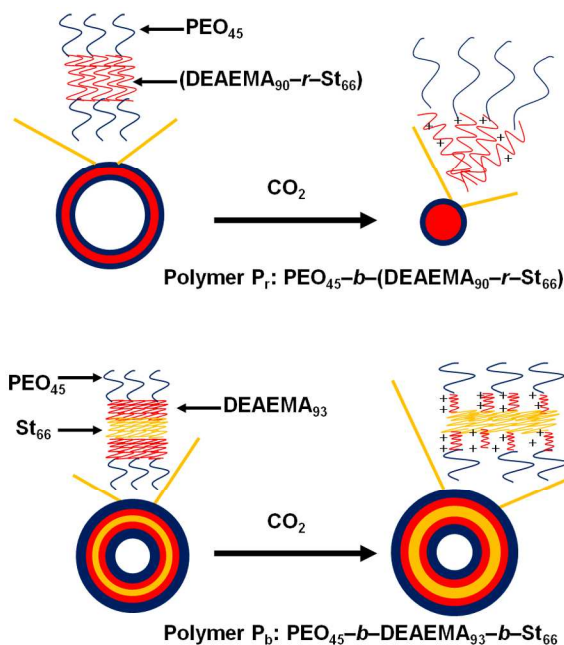


Fig. 7 Cryo-TEM photographs of the aggregates for the triblock counterpart **P_b**, before (a) and after (b) CO₂ treatment. The sample is free of staining. Bars: 50 nm.

For the counterpart triblock copolymer **P_b**, typical vesicles with light membrane and dark hollow volume can be observed as well before and after bubbling CO₂ with cryo-TEM technique (Fig. 7). And the average diameter is about 343 and 405 nm, respectively. The vesicle shows an expansion after reaction with CO₂ instead of collapse into small spherical micelle, being consistent with the DLS results (Fig. 5).



Scheme 2 Schematic representation of CO₂ induced vesicle to spherical micelle transition (top) for random copolymer **P_r**, as well as the vesicles formed by the triblock counterpart **P_b** (bottom).

After figuring out the different morphology of copolymer **P_r** and **P_b**, we expected to comprehend the mechanism on how CO₂ drives the different morphologic change. Based on the protonated degree, we attempted to rationalize morphologic transition with the theory of hydrophilic volume fraction (f_{philic}) proposed by Discher,¹ but failed (Table S1). Recently, Zhao and co-workers developed a series of morphologic transformation with triblock copolymer and proposed a model of restricted hydration to explain the re-shape behaviour of the assemblies.¹⁴ This restricted hydration theory is helpful for the understanding of the vesicle to micelle transition in the present work. Before CO₂ treatment, the random copolymer **P_r** acts like a two-block structure with hydrophobic segment DEAEMA_{90-r}-St₆₆ and a hydrophilic block of PEO₄₅, since the DEAEMA is hydrophobic in the original state without CO₂ treatment. Thus the **P_r** aggregates into a three-layer structure (Scheme 2, top) in water. After reaction with CO₂, a portion of DEAEMA moieties become protonated and convert to charged species. However, because of the intensive steric hindrance effect from the adjacent St groups in the random segment, the remaining non-protonated DEAEMA cannot be charged any more. This explains why the protonated degree of random copolymer is as low as 35% after treatment of CO₂. The charge species cannot dissolve freely, in other words, the hydration of protonated DEAEMA is restricted but the electrostatic repulsion results in an increase of the interfacial free energy, which drives the vesicle to change its morphology to reduce the accumulated energy, resulting in the formation of small-sized spherical micelles. But for the counterpart triblock copolymer **P_b** with an entire three-block structure, it would aggregate into a five-layer structure (Scheme 2, bottom) in water, since the St block and DEAEMA block separate into two micro-phases. The protonation of DEAEMA moieties is not influenced by the St blocks and the hydration of DEAEMA block is free of limitation, which results in faster protonation process and a

higher level of protonated degree up to 97%. So the interfacial free energy does not increase significantly, which can be offset by an expansion, avoiding the extreme morphologic transformation. This mechanism can be supported by some experimental results. Firstly, the protonated (or charged) state of DEAEEMA is demonstrated by the conductivity increase and pH decrease upon the stimulus of CO₂. Secondly, the different protonated degrees, 35% for P_r and 97% for P_b, prove the existence of restrict effect in P_r but not in P_b. What is more, even after ultrasonic treatment, the protonated degree of P_r remains at 39% upon CO₂ stimulus, and the vesicle to sphere transition occurs as well (Fig. S7), further demonstrating the strong restriction. We should mention that the reverse morphologic transition from spherical micelle to vesicle seems hard to reach (Fig. S8) for the random copolymer, which might be also related with the steric hindrance.

Conclusions

In conclusion, a CO₂-driven vesicle to spherical micelle morphologic regulation was demonstrated based on a random copolymer with a hydrophilic segment. As a contrast, its triblock copolymer counterpart with similar polymerization degree of hydrophobic monomers gives no significant morphologic change except for an expansion. The restrict hydration of the CO₂-responsive moieties caused by the adjacent groups in the random structure should be responsible for the morphologic transformation. This random strategy may offer a new way to design and realize precise morphologic manipulation. Considering the good biocompatibility and membrane permeability of CO₂ as a new trigger, this morphologic transition have potential application in biotherapy as well.

Acknowledgements

The authors would like to thank the financial support from the National Natural Science Foundation of China (21273223, 21173207), and the Distinguished Youth Fund of Sichuan Province (2010JQ0029). We also thank Dr. Xiaojun Huang and Dr. Gang Ji for technical support in cryo-TEM characterization and gratefully acknowledge the use of cryo-TEM facilities at the Center for Biological Imaging (CBI), Institute of Biophysics, Chinese Academy of Sciences.

Notes and references

^a Chengdu Institute of Organic Chemistry, Chinese Academy of Sciences, Chengdu 610041, P. R. China.

^b Polymer Research Institute, State Key Laboratory of Polymer Materials Engineering, Sichuan University, Chengdu 610065, P. R. China. Tel. &

Fax: +86 (0)28 8540 8037; E-mail: yjfeng@scu.edu.cn

^c University of Chinese Academy of Sciences, Beijing 100049, P. R. China.

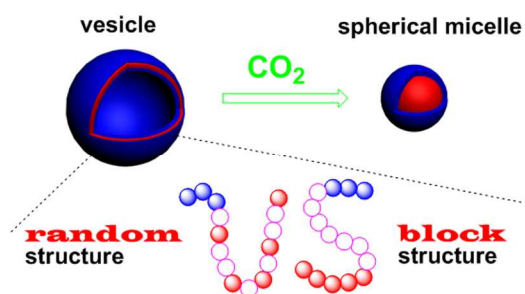
† Electronic Supplementary Information (ESI) available: ¹H NMR spectra, pK_a measurement, calculation of protonated degree (δ) and average sequence length, and additional results. See DOI: 10.1039/b000000x/

1. D. E. Discher and A. Eisenberg, *Science*, 2002, **297**, 967–973.
2. A. Blanz, S. P. Armes and A. J. Ryan, *Macromol. Rapid Commun.*, 2009, **30**, 267–277.
3. J. Du and R. K. O'Reilly, *Soft Matter*, 2009, **5**, 3544–3561.

4. D. E. Discher and F. Ahmed, in *Annu. Rev. Biomed. Eng.*, 2006, **8**, 323–341.
5. A. Sundararaman, T. Stephan and R. B. Grubbs, *J. Am. Chem. Soc.*, 2008, **130**, 12264–12265.
6. M.-H. Li and P. Keller, *Soft Matter*, 2009, **5**, 927–937.
7. J. Z. Du and S. P. Armes, *J. Am. Chem. Soc.*, 2005, **127**, 12800–12801.
8. Y. Morishima, *Angew. Chem., Int. Ed.*, 2007, **46**, 1370–1372.
9. Q. Yan, J. Y. Yuan, Z. N. Cai, Y. Xin, Y. Kang and Y. W. Yin, *J. Am. Chem. Soc.*, 2010, **132**, 9268–9270.
10. E. G. Bellomo, M. D. Wyrsta, L. Pakstis, D. J. Pochan and T. J. Deming, *Nat. Mater.*, 2004, **3**, 244–248.
11. M. A. C. Stuart, W. T. S. Huck, J. Genzer, M. Muller, C. Ober, M. Stamm, G. B. Sukhorukov, I. Szleifer, V. V. Tsukruk, M. Urban, F. Winnik, S. Zauscher, I. Luzinov and S. Minko, *Nat. Mater.*, 2010, **9**, 101–113.
12. A. O. Moughton and R. K. O'Reilly, *Chem. Commun.*, 2010, **46**, 1091–1093.
13. Q. Jin, C. Luy, J. Ji and S. Agarwal, *J. Polym. Sci., Part A: Polym. Chem.*, 2012, **50**, 451–457.
14. Q. Yan and Y. Zhao, *J. Am. Chem. Soc.*, 2013, **135**, 16300–16303.
15. A. O. Moughton, J. P. Patterson and R. K. O'Reilly, *Chem. Commun.*, 2011, **47**, 355–357.
16. H. W. Shen, L. F. Zhang and A. Eisenberg, *J. Am. Chem. Soc.*, 1999, **121**, 2728–2740.
17. K. E. B. Doncom, C. F. Hansell, P. Theato and R. K. O'Reilly, *Polym. Chem.*, 2012, **3**, 3007–3015.
18. X. Liu and M. Jiang, *Angew. Chem., Int. Ed.*, 2006, **45**, 3846–3850.
19. J. Z. Du, H. Y. Long, Y. Y. Yuan, M. M. Song, L. Chen, H. Bi and J. Wang, *Chem. Commun.*, 2012, **48**, 1257–1259.
20. O. Uzun, A. Sanyal, H. Nakade, R. J. Thibault and V. M. Rotello, *J. Am. Chem. Soc.*, 2004, **126**, 14773–14777.
21. Y. X. Liu, P. G. Jessop, M. Cunningham, C. A. Eckert and C. L. Liotta, *Science*, 2006, **313**, 958–960.
22. Z. R. Guo, Y. J. Feng, Y. Wang, J. Y. Wang, Y. F. Wu and Y. M. Zhang, *Chem. Commun.*, 2011, **47**, 9348–9350.
23. P. G. Jessop, S. M. Mercer and D. J. Heldebrant, *Energy Environ. Sci.*, 2012, **5**, 7240–7253.
24. Z. R. Guo, Y. J. Feng, S. He, M. Z. Qu, H. L. Chen, H. B. Liu, Y. F. Wu and Y. Wang, *Adv. Mater.*, 2013, **25**, 584–590.
25. A. J. Morse, D. Dupin, K. L. Thompson, S. P. Armes, K. Ouzineb, P. Mills and R. Swart, *Langmuir*, 2012, **28**, 11733–11744.
26. F. E. Karet, *Nephron Physiol.*, 2011, **118**, 28–34.
27. Q. Yan, R. Zhou, C. Fu, H. Zhang, Y. Yin and J. Yuan, *Angew. Chem., Int. Ed.*, 2011, **50**, 4923–4927.
28. Q. Yan and Y. Zhao, *Angew. Chem., Int. Ed.*, 2013, **52**, 9948–9951.
29. Q. Yan, J. Wang, Y. Yin and J. Yuan, *Angew. Chem., Int. Ed.*, 2013, **52**, 5070–5073.
30. B. Yan, D. H. Han, O. Boissiere, P. Ayotte and Y. Zhao, *Soft Matter*, 2013, **9**, 2011–2016.
31. K. Feng, N. Xie, B. Chen, L.-P. Zhang, C.-H. Tung and L.-Z. Wu, *Macromolecules*, 2012, **45**, 5596–5603.
32. J. Guo, Y. Zhou, L. Qiu, C. Yuan and F. Yan, *Polym. Chem.*, 2013, **4**, 4004–4009.
33. A. Honglawan, H. Ni, D. Weissman and S. Yang, *Polym. Chem.*, 2013, **4**, 3667–3675.
34. K. Dan, N. Bose and S. Ghosh, *Chem. Commun.*, 2011, **47**, 12491–12493.
35. K. Dan, P. Rajdev, J. Deb, S. S. Jana and S. Ghosh, *J. Polym. Sci., Part A: Polym. Chem.*, 2013, **51**, 4932–4943.
36. X. Liu, J.-S. Kim, J. Wu and A. Eisenberg, *Macromolecules*, 2005, **38**, 6749–6751.
37. X. W. Xu, A. E. Smith, S. E. Kirkland and C. L. McCormick, *Macromolecules*, 2008, **41**, 8429–8435.
38. A. J. Convertine, D. S. W. Benoit, C. L. Duvall, A. S. Hoffman and P. S. Stayton, *J. Control. Release*, 2009, **133**, 221–229.
39. A. P. Francis, D. H. Solomon and T. H. Spurling, *J. Macromol. Sci., Chem.*, 1974, **A8**, 469–476.
40. Y. Xu, Q. Xu, J. Lu, X. Xia and L. Wang, *Polym. Bull.*, 2007, **58**, 809–817.

-
41. Z. Cheng, X. Zhu, N. Zhou, J. Zhu and Z. Zhang, *Radiat. Phys. Chem.*, 2005, **72**, 695-701.
 42. Y. M. Zhang, Y. J. Feng, J. Y. Wang, S. He, Z. R. Guo, Z. L. Chu and C. A. Dreiss, *Chem. Commun.*, 2013, **49**, 4902–4904.
 - s 43. Y. M. Zhang, Y. J. Feng, Y. J. Wang and X. L. Li, *Langmuir*, 2013, **29**, 4187–4192. ¹⁰

Table of Content:



5 A vesicle to spherical micelle morphologic regulation has been demonstrated with a random copolymer rather than its triblock counterpart.